HHS Public Access

Author manuscript

Neuroimage. Author manuscript; available in PMC 2025 February 15.

Published in final edited form as:

Neuroimage. 2025 February 01; 306: 121018. doi:10.1016/j.neuroimage.2025.121018.

The polarity of high-definition transcranial direct current stimulation affects the planning and execution of movement sequences

Jake J. Son[a,b,1], **Tara D. Erker**[a,1], **Thomas W. Ward**[a,c], **Yasra Arif**[a], **Peihan J. Huang**[a,c], **Jason A. John**[a], **Kellen M. McDonald**[a,c], **Nathan M. Petro**[a], **Grant M. Garrison**[a], **Hannah J. Okelberry**[a], **Kennedy A. Kress**[a], **Giorgia Picci**[a,c], **Elizabeth Heinrichs-Graham**[a,b,c], **Tony W. Wilson**[a,b,c,*]

[a] Institute for Human Neuroscience, Boys Town National Research Hospital, Boys Town, NE, USA

[b] College of Medicine, University of Nebraska Medical Center, Omaha, NE, USA

[c] Department of Pharmacology & Neuroscience, Creighton University, Omaha, NE, USA

Abstract

Noninvasive brain stimulation of the primary motor cortex has been shown to alter therapeutic outcomes in stroke and other neurological conditions, but the precise mechanisms remain poorly understood. Determining the impact of such neurostimulation on the neural processing supporting motor control is a critical step toward further harnessing its therapeutic potential in multiple neurological conditions affecting the motor system. Herein, we leverage the excellent spatio-temporal precision of magnetoencephalographic (MEG) imaging to identify the spectral, spatial, and temporal effects of high-definition transcranial direct current stimulation (HD-tDCS) on the neural responses supporting motor control. Participants (N = 67) completed three HD-tDCS visits (anode, cathode, sham), with each involving 20 min of left primary motor cortex stimulation and performance of a simple/complex motor sequencing task during MEG. Whole-brain statistical analyses of beta oscillatory responses revealed stimulation-by-task interaction effects in the left primary motor cortex, right occipitotemporal, and the right dorsolateral prefrontal cortices.

* Corresponding author at: Institute for Human Neuroscience, Boys Town National Research Hospital, Omaha, NE 68010, USA. tony.wilson@boystown.org (T.W. Wilson).

[1]These authors contributed equally

Declaration of competing interest

The authors of this manuscript acknowledge no conflicts of interest, financial or otherwise.

CRediT authorship contribution statement

Jake J. Son: Writing – review & editing, Writing – original draft, Visualization, Methodology, Formal analysis, Data curation, Conceptualization. **Tara D. Erker:** Writing – review & editing, Writing – original draft, Visualization, Methodology, Formal analysis, Data curation, Conceptualization. **Thomas W. Ward:** Writing – review & editing, Methodology, Formal analysis, Conceptualization. **Yasra Arif:** Writing – original draft, Methodology, Conceptualization. **Peihan J. Huang:** Writing – review & editing, Methodology, Conceptualization. **Jason A. John:** Writing – review & editing, Project administration, Data curation. **Kellen M. McDonald:** Writing – review & editing, Data curation. **Nathan M. Petro:** Writing – review & editing, Data curation. **Grant M. Garrison:** Writing – review & editing, Project administration, Data curation. **Hannah J. Okelberry:** Writing – review & editing, Project administration, Data curation. **Kennedy A. Kress:** Writing – review & editing, Project administration, Data curation. **Giorgia Picci:** Writing – review & editing, Data curation. **Elizabeth Heinrichs-Graham:** Writing – review & editing, Supervision, Conceptualization. **Tony W. Wilson:** Writing – review & editing, Visualization, Supervision, Resources, Methodology, Investigation, Funding acquisition, Conceptualization.

Broadly, anodal stimulation induced significantly stronger beta oscillatory responses in these regions during simple movement sequences, while neural responses to complex sequences were not affected by stimulation. En masse, these data suggest that the beta oscillations serving motor planning (i.e., pre-movement) are particularly sensitive to the polarity of noninvasive stimulation and that the impact varies based on the difficulty of the movement sequence.

Keywords

Beta ERD; Magnetoencephalography; Primary motor cortex; dlPFC; MEG; Oscillations

1. Introduction

Motor control is essential to everyday functioning and is affected by aging, psychopathology, and neurological disorders, including Parkinson's disease, multiple sclerosis, and cerebellar ataxia. Noninvasive brain stimulation techniques present a possible therapeutic approach to normalizing motor control in these conditions, with several recent studies reporting at least moderate success in such areas (Nombela-Cabrera et al., 2023; Qiu et al., 2023; Wang et al., 2021). However, the field's limited understanding of how noninvasive brain stimulation affects motor control in healthy adults remains a major barrier to progress in this area. In contrast, there is a large body of literature that extensively characterizes the neurophysiology of motor control in healthy adults and children. These studies have shown that prior to and during movement, there is a robust event-related desynchronization (ERD), or decrease in oscillatory power relative to the baseline, in the beta frequency range (approximately 15–30 Hz) within the motor cortex contralateral to movement (and to a lesser magnitude, the ipsilateral motor cortex). This oscillatory response is followed by a post-movement beta rebound (PMBR) that is tightly yoked to movement offset and is located slightly posterior to the beta ERD (Heinrichs-Graham et al., 2016, 2017, 2018; Jurkiewicz et al., 2006; Wiesman et al., 2020; Wilson et al., 2010). There is considerable evidence that the neural oscillatory dynamics supporting planning and execution in the beta range are dissociable and index distinct elements of motor control in movement sequencing tasks (Heinrichs-Graham et al., 2018; Heinrichs-Graham and Wilson, 2015; Spooner et al., 2021; Ward et al., 2023; Ng et al., 2011; Pfurtscheller and Lopes da Silva, 1999; Tzagarakis et al., 2010; Wilson et al., 2014). Indeed, beta oscillatory responses linked with movement planning are present during motor imagery tasks, even when no movement is completed (Brinkman et al., 2014). Various movement parameters have also been shown to modulate the amplitude of the beta ERD, including task difficulty, where greater complexity has been linked to stronger beta ERD responses during the execution phase (Heinrichs-Graham and Wilson, 2015), and response uncertainty, where greater uncertainty has been associated with weaker beta ERD responses during the planning stage (Tzagarakis et al., 2010).

The amplitude of the beta ERD can also be modulated through transcranial direct current stimulation (tDCS), with preliminary evidence that anodal stimulation strengthens the beta ERD (Notturno et al., 2014). Such noninvasive brain stimulation techniques are known to change the excitability of local neuronal populations (Liebetanz et al., 2002; Nitsche

et al., 2003; Nitsche and Paulus, 2001), although the precise mechanisms are not fully understood. Many studies have suggested that tDCS alters the local ionic environment, which affects the response threshold of surrounding neural populations, but does not induce action potentials (Liebetanz et al., 2002; Nitsche et al., 2003; Nitsche and Paulus, 2001). To increase the spatial specificity of such effects, some recent studies have used a small array of metal electrodes (i.e., high-definition tDCS (HD-tDCS)) rather than the conventional tDCS sponges, which have been shown to cause widespread effects as the induced electric field is diffuse (Datta et al., 2009; Edwards et al., 2013). Regardless of the focality, the polarity of stimulation has been shown to cause differential effects, with anodal stimulation being associated with increases in motor excitability and cathodal stimulation being associated with decreases in excitability (Antal et al., 2007; Nitsche and Paulus, 2000; Saucedo Marquez et al., 2013). Both anodal and cathodal stimulation can cause changes in behavioral performance (Antal et al., 2007; Hodkinson et al., 2022), which vary based on the specific task and the stimulation parameters (Saucedo Marquez et al., 2013). In many past studies, tDCS of the primary motor cortex has been shown to modulate neuronal responses and have favorable effects, such as improvements in motor learning and enhanced dexterity (Bastani and Jaberzadeh, 2014; Convento et al., 2014; Guimarães et al., 2023).

A distributed network of cortical regions extending beyond the primary motor cortex is known to support motor control, including the posterior parietal cortex, dorsolateral prefrontal cortex (dlPFC), and cerebellum (Hanakawa et al., 2008; Kim et al., 2018; Toni et al., 1998). These regions are known to be sensitive to the complexity of movement sequences and together may also support the increased motor coordination and execution demands involved in performing motor sequences (Heinrichs-Graham and Wilson, 2015). Thus, alterations in non-primary motor areas may impact network level connectivity and functioning across various nodes of the motor control network. For instance, tDCS studies of the dlPFC have demonstrated significant effects on motor sequence learning and other aspects of motor task performance, which supports a connection between higher-order association cortices and motor function (Ballard et al., 2021; Leite et al., 2011). Further, the prefrontal, anterior cingulate, and parietal cortices exhibit complementary profiles of neural activity during motor sequence learning and play a clear role in supporting motor control of complex movements (Toni et al., 1998). However, there is a paucity of studies examining the impact of stimulation over the primary motor cortex on neural dynamics across the distributed network of brain regions supporting motor control.

Herein, we investigated whether HD-tDCS of the primary motor cortex affects the neural oscillations serving the planning and execution of motor actions in healthy young adults using a whole-brain approach. Specifically, we applied anodal and cathodal HD-tDCS and then collected magnetoencephalography (MEG) during a motor sequencing paradigm. We chose to stimulate the primary motor cortex as studies have shown it is critical to motor control during movement sequences and is strongly interconnected to critical regions in the parietal and dlPFC (Ballard et al., 2021; Heinrichs-Graham and Wilson, 2015; Leite et al., 2011; Nakashima et al., 2021). Based on previous studies that stimulated the primary motor cortex (Nitsche and Paulus, 2000; Stagg and Nitsche, 2011), we hypothesized that there would be polarity-dependent modulation of motor planning and execution dynamics that would vary based on the complexity of the sequence. Specifically, we predicted that anodal

stimulation would strengthen the beta ERD while cathodal stimulation would weaken the beta ERD in the primary motor cortex. Further, we anticipated association cortices to be more significantly impacted by neurostimulation during the planning phase relative to the execution phase.

2. Methods

2.1. Ethical approval

All experimental procedures conformed to the standards set by the *Declaration of Helsinki.* The study protocol was approved by the local Institutional Review Board (IRB). A full description of the study was given to all participants, followed by written informed consent, which adhered to the guidelines set forth by the IRB.

Participants—Sixty-seven, right-handed healthy adults (33 females) between the ages of 19 – 34 years (mean = 25.2 years) were enrolled from the local community. Exclusionary criteria included any medical illness affecting CNS function (e.g., HIV/AIDS), any neurological or psychiatric disorder, history of head trauma, current substance use, and the MEG laboratory's standard exclusionary criteria (e.g., ferromagnetic implants). All experimental procedures conformed to the standards set by the *Declaration of Helsinki.*

2.2. High-definition transcranial direct current stimulation

A 4 × 1 configuration (central electrode surrounded by four with opposite polarity; Soterix Medical; New York, NY) was utilized to deliver HD-tDCS to the left primary motor cortex (M1). Based on the Okamoto et al. transformations of the scalp-based international 10/20 system to MNI space, the central electrode was placed on C3, which corresponds to the primary motor cortex, with the surrounding electrodes of opposite polarity at C1, C5, FC3, CP3 (Klem et al., 1999; Okamoto et al., 2004; Okamoto and Dan, 2005). This montage was designed to deliver maximum stimulation to the left primary motor cortex (i.e., M1) with the least possible stimulation spreading to neighboring regions. Current flow modeling was conducted with the ROAST software to ensure the stimulation was being applied to the intended region with minimal spread (Fig. 1; Huang et al., 2019).

Each participant completed three separate visits at the same time of day, but at least one week apart (M = 9.77 days, std = 5.94 days). Stimulation conditions were pseudorandomized to include two active (i.e., anodal and cathodal) and one sham HD-tDCS session. Participants, as well as the researchers who analyzed the data, were kept blind as to which visits were active stimulations and sham. Staff members applying the stimulation were not blinded to the experimental conditions of each visit, but had no role in data analysis or MEG data acquisition. During the active visits, participants underwent 20 min of 2.0 mA direct current stimulation, plus a 30-s ramp-up period. No stimulation was applied during the sham visits besides that of the ramping procedure, which was adopted to mitigate the likelihood of participants accurately identifying which session they were undergoing. To keep them actively engaged, participants performed a multi-source interference task during the stimulation session, which was designed to probe cognitive control and engage attention networks (Arif et al., 2023, 2024; Bush et al., 2003; Bush and Shin, 2006; Son et al., 2024;

Wiesman et al., 2020; Wiesman and Wilson, 2020). Following active/sham stimulation, participants were moved to the MEG recording chamber, with about 45 min from the end of stimulation to the beginning of the MEG experiment which is well within the time window to monitor offline tDCS effects (Kuo et al., 2013).

2.3. Experimental paradigm

This study utilized a motor sequencing task designed by and previously used in our laboratory (Heinrichs-Graham and Wilson, 2015; McCusker et al., 2021; Ward et al., 2023). The participant was asked to fixate on a centrally presented crosshair for 3750 ms with their hand resting on a five-finger button pad. After this baseline period, a series of three numbers, each corresponding to a finger on their hand, was presented on the screen. Participants were instructed to press the buttons corresponding to the sequence. Participants had 2250 ms to complete their movement, after which the numbers disappeared, leaving only the fixation cross remaining on the screen. There were two conditions that were distinguished by the complexity of the motor plan (Fig. 1). In the "simple" condition, the series of numbers in the plan were sequential and resulted in the tapping of 3 adjacent fingers (i.e., "1–2–3″, "2–3–4″, "4–3–2″, "3–2–1″). In the "complex" condition, each number was at least one number away from the previous number (i.e., "1–4–2″, "2–4–1″, "3–1–4″, "4–1–3″), and thus mapped to a sequence in which the finger being tapped was not adjacent to the previous finger tapped. Trials were pseudo-randomized and a total of 160 trials (80 per condition) were completed, with an overall MEG recording time of about 16 min for the task.

2.4. MEG data acquisition

All recordings were conducted in a two-layer magnetically shielded VACOSHIELD room (Vacuumschmelze, Hanau, Germany). With an acquisition bandwidth of 0.1–330 Hz, neuromagnetic responses were sampled continuously at 1 kHz using a MEGIN Neo MEG system (Helsinki, Finland) with 306 sensors, including 204 planar gradiometers and 102 magnetometers. During data acquisition, participants were monitored via real-time audio-visual feeds from inside the shielded room. Each MEG dataset was individually corrected for head motion and subjected to noise reduction using the signal space separation method with a temporal extension (Taulu et al., 2005; Taulu and Simola, 2006).

2.5. Structural MRI processing and MEG coregistration

Prior to MEG measurement, five coils were attached to the participant's head and localized, together with the three fiducial points and scalp surface, with a 3D digitizer (FASTRAK, Polhemus Navigator Sciences, Colchester, VT, USA). Once participants were positioned for MEG recording, an electric current with a unique frequency label (e.g., 322 Hz) was fed to each of the coils. This induced a measurable magnetic field and allowed each coil to be localized in reference to the sensors throughout the recording session. As coil locations were also known with respect to head coordinates, all MEG measurements could be transformed into a common coordinate system. With this coordinate system, each participant's MEG data were coregistered with their high-resolution T1-weighted structural brain data prior to source space analysis using BESA MRI (Version 2.0). Structural T1-weighted MR images were acquired using a Siemens Prisma 3T MRI scanner with a 32-channel head coil and a 3D MP-RAGE sequence with the following parameters: TR = 2400 ms; TE = 2.05 ms;

flip angle = 8○; FOV = 256 mm; slice thickness = 1 mm; voxel size = 1 mm3; 192 slices. Structural MRI data were transformed into standardized space and aligned parallel to the anterior and posterior commissures. Following source analysis, each participant's MEG functional images were also transformed into standardized space and spatially resampled.

2.6. MEG pre-processing, time-frequency transformation, and sensor-level statistics

Eye blinks and cardio-artifacts were removed from the data using signal space projection (SSP), which was accounted for during source reconstruction (Uusitalo and Ilmoniemi, 1997). The continuous magnetic time series was divided into epochs (duration: 5400 ms), with 0 ms defined as movement onset (i.e., first button press) and the baseline defined as the −1400 to −900 ms time window (i.e., before movement onset). Epochs containing artifacts were removed based on a fixed threshold method, supplemented with visual inspection. Briefly, the amplitude and gradient distributions across all trials were determined per participant, and those trials containing the highest amplitude and/or gradient values relative to this distribution were rejected based on participant-specific thresholds. This approach was employed to minimize the impact of individual differences in sensor proximity and head size, which strongly affect MEG signal amplitude. After artifact rejection, an average of 70.30 (std = 8.31) epochs in the simple and 69.68 (std = 8.70) epochs in the complex condition remained. A 2 × 3 repeated-measures analysis of variance (ANOVA) indicated that the number of trials did not differ by condition ($p = .106$), by stimulation ($p = .187$), or the interaction ($p = .289$).

Artifact-free epochs were transformed into the time-frequency domain using complex demodulation (Kovach and Gander, 2016), and the resulting spectral power estimations per sensor were averaged over trials to generate time-frequency plots of mean spectral density. This time-frequency analysis was performed with a frequency-step of 2 Hz and a time-step of 25 ms between 4 and 30 Hz to examine beta activity. These sensor-level data were normalized using the respective bin's baseline power, which was calculated as the mean power during the −1400 to −900 ms time window. The specific time-frequency windows used for source reconstruction were determined by statistical analysis of the sensor level spectrograms across all participants and stimulation conditions using the entire array of 204 gradiometers. Specifically, paired-sample *t*-tests against baseline were run on each data point, and the output spectrogram of t-values was thresholded at $p < .05$ to define time-frequency bins containing potentially significant oscillatory deviations across all participants and stimulation conditions. Time-frequency bins that survived the threshold were then clustered with temporally and/or spectrally neighboring bins that were also above the threshold ($p < .05$), and a cluster value was derived by summing the t-values of all data points in the cluster. Nonparametric permutation testing (1000 permutations) was then used to derive a distribution of cluster values, and the significance level of the observed clusters was tested directly using this distribution (Ernst, 2004; Maris and Oostenveld, 2007).

2.7. MEG beamformer imaging and statistics

Cortical neural responses were imaged using the dynamic imaging of coherent sources (DICS) beamformer (Gross et al., 2001; Van Veen et al., 1997), which employs spatial filters in the time-frequency domain to calculate source power for the entire brain

volume. Such images are typically referred to as pseudo-t maps, with units (pseudo-t) that reflect noise-normalized power differences (i.e., active vs. passive) per voxel. MEG preprocessing and imaging used the Brain Electrical Source Analysis (BESA; Version 7.1) software. Normalized source power was computed for the selected time frequency windows (see Results) over the entire brain volume per participant at 4.0 mm × 4.0 mm × 4.0 mm resolution. The resulting beamformer images were grand-averaged across all participants and HD-tDCS configurations (i.e., anodal, cathodal, and sham) to assess the neuroanatomical basis of the significant oscillatory responses identified through the MEG sensor-level analysis. For a more detailed description of our methods, see (Wiesman and Wilson, 2020). These beamformer images were subjected to whole-brain statistical analyses using a 2 × 3 repeated-measures ANOVA, separately for planning and execution windows. The condition factor had two levels (simple, complex) and the stimulation factor had three levels (sham, anodal, cathodal). Any beamforming outliers for each time-frequency window of interest were excluded prior to analysis.

3. Results

3.1. Behavioral results

For each participant, reaction time, movement duration, and accuracy measures were calculated and tested for main effects and stimulation-by-task interactions. Participants completed the motor sequencing task with a high degree of accuracy, with an average of 94.02 % across stimulation and task conditions (see Table 1 for more details). All statistical analyses were conducted after removing outliers that were three standard deviations from the mean. For accuracy, there was a significant main effect of task condition ($F(1, 58) = 5.36$, $p = .024$), such that participants were less accurate in the complex relative to the simple condition. Further, there was a main effect of task condition on reaction time ($F(2, 61) = 93.04$, $p < .001$) and reaction time variability ($F(1, 61) = 5.14$, $p = .027$; Fig. 2), such that participants took longer to respond and were less variable (i.e., lower coefficient of variation) in the complex compared to the simple condition. There was also a main effect of task condition on movement duration ($F(1, 63) = 99.99$, $p < .001$), such that participants took longer and were more variable in completing the full movement sequence in the complex relative to the simple condition (Fig. 2). There was no main effect of task condition on movement duration variability ($F(1, 63) = 1.223$, $p = .273$). No main effects of stimulation or interaction effects were found for reaction time, accuracy, or measures of variability.

3.2. Sensor-level results

Using a rigorous two-step approach to determining time-frequency windows, we identified statistically significant oscillatory responses in the beta range (16–24 Hz) centered around the button press (Fig. 3). All responses were significant at $p < .005$ following multiple comparisons correction using nonparametric cluster-based permutation testing. The beta ERD response was separated into the planning (−500 to 0 ms) and execution (0 to 500 ms) phases to distinguish the differential cognitive and motor processes that serve the initiation of motor sequences. The neural generators of these time-frequency responses were estimated using a beamformer algorithm, separately for each task and stimulation condition. These

images were averaged across all task and stimulation conditions per person, then grand averaged across the sample to generate images representative of the group-level response in each time-frequency window (Fig. 3). Note that the PMBR response is also clearly discernable in Fig. 3, but this response was not imaged or further examined given the significant conditional differences in movement duration that were observed, as this would confound any comparisons.

3.3. Dynamic functional maps: main effects of task condition

Two (planning and execution) 2 × 3 repeated-measures ANOVAs indicated a main effect of task condition in both the planning and execution phases (all ps < 0.001, k-threshold = 8). In the planning phase, participants exhibited a stronger beta ERD response (i.e., more negative relative to baseline) in the complex relative to the simple condition in the right somatosensory cortices ($F(1, 43) = 26.05$) and right superior parietal cortex (($F(1, 43) = 19.36$; Supplemental Figure 1). In contrast, the right inferior occipital ($F(1, 43) = 14.86$) and right occipitotemporal regions ($F(1, 43) = 15.97$) exhibited stronger beta ERD responses in the simple relative to the complex condition. During the execution phase, participants exhibited stronger beta ERD responses in the complex relative to the simple condition in the left superior temporal cortex ($F(1, 43) = 16.84$), anterior medial prefrontal cortex (amPFC; $F(1, 43) = 16.60$), and a distributed network of brain regions that included the occipito/parietal/temporal cortices ($F(1, 43) = 63.68$). There were no significant main effects of stimulation condition in either the planning or execution windows.

3.4. Dynamic functional maps: stimulation-by-task interaction effect

In addition to the main effects described above, we found stimulation by task interaction effects in both the planning and execution windows (all ps < 0.001, k-threshold = 8). During the planning phase (Fig. 4), post-hoc testing revealed stronger beta ERD responses (i.e., more negative relative to baseline) during simple trials in the right dlPFC ($F(2, 86) = 10.08$) following anodal stimulation compared to both cathodal ($p < .001$) and sham ($p = .003$) conditions, while the cathode and sham conditions did not differ from one another ($p = .151$). This overall pattern in the right dlPFC was maintained during the movement execution window ($F(2, 86) = 8.52$), with post-hoc testing again revealing stronger beta oscillations during simple trials following anodal stimulation compared to both cathode ($p = .004$) and sham ($p = .049$) conditions, while the cathode and sham conditions did not differ from one another ($p = .502$; Fig. 4). Further, beyond the dlPFC, the same pattern held for motor planning beta responses in a medial area of the left primary motor cortex that bordered the supplementary motor area ($F(2, 86) = 10.20$) and right occipitotemporal cortex ($F(2, 86) = 8.34$). Briefly, post hoc analyses revealed stronger beta ERD responses (i.e., more negative relative to baseline) in the left primary motor cortex during simple trials following anodal stimulation compared to both cathodal ($p = .002$) and sham ($p = .039$) conditions, with the latter two stimulation conditions not differing from each other ($p = .444$). Finally, in the right occipitotemporal cortex post-hoc testing revealed that in the simple condition, anodal stimulation was associated with stronger beta ERD responses compared to the cathode ($p = .036$) and sham ($p = .006$) conditions, while the cathode and sham conditions did not differ from one another ($p = .477$; Fig. 4). In addition, anodal stimulation was associated with weaker beta ERD responses compared to the sham ($p = .027$) but not the cathodal condition

(p = .128) during complex trials, while the sham and cathode conditions did not differ from one another (p = .283).

4. Discussion

In this investigation, we used high-definition transcranial direct current stimulation (HD-tDCS) and high-density MEG imaging to quantify movement-related neural dynamics that were differentially sensitive to stimulation polarity and movement complexity. We identified several main effects of task condition in the motor planning and execution windows, with the overall pattern being that complex movements elicit stronger beta ERD in both the planning and execution windows across a distributed network of brain regions involved in basic sensory, motor, and higher-order processing. Our most interesting findings were the stimulation-by-task interaction effects in the left primary motor cortex (i.e., direct target of stimulation), the right dorsolateral prefrontal cortex (dlPFC), and the right occipitotemporal cortex. Functionally, the beta ERD is tightly coupled with the planning and execution of movements and dissipates quickly following the completion of a movement sequence. These neural responses occur specifically in brain regions that are interconnected and critical for motor control. Indeed, altered beta ERD responses have been identified across disorders with motor deficits and are frequently correlated with the severity of symptoms (Embury et al., 2019; Heinrichs-Graham et al., 2014a,b, 2017; McCusker et al., 2021; Wilson et al., 2013, 2016). This pattern of findings suggests that the beta ERD responses supporting movement planning and execution are sensitive to the polarity of noninvasive electrical stimulation and that these neuromodulatory effects are contingent on the complexity of the movement sequence.

4.1. Behavioral findings

In line with the existing literature, we identified a main effect of task condition behaviorally, such that participants took longer to initiate (i.e., reaction time) and complete (i.e., movement duration) the movement sequences in the complex relative to the simple condition (Haaland et al., 2004; Heinrichs-Graham and Wilson, 2015; McCusker et al., 2021; Ward et al., 2023). Furthermore, there was a significant difference in reaction time variability (i.e., coefficient of variation), such that participants were more variable in movement initiation in the simple relative to the complex condition. However, there was no condition-wise difference in variability in the duration of the sequential movement. While movement variability and the speed-accuracy tradeoff (i.e., Fitts' law) have been examined in rapid aimed movements, linking these processes to target localization, movement preparation time, movement execution, and the variability of more fine-tuned digit movements remains relatively unexplored (Churchland et al., 2006; Sutter et al., 2021; van Beers et al., 2004). Our novel results suggest that the variability of movement planning, but not execution of finger movements, is susceptible to the complexity of the movement sequence. Interestingly, we did not observe a main effect of stimulation on behavioral measures. The literature is mixed with respect to the impact of brain stimulation on motor performance, with repetitive transcranial magnetic stimulation (rTMS) of the motor cortices impacting temporal but not spatial accuracy (Avanzino et al., 2008) and behavioral outcomes in complex but not simple conditions (Gerloff et al., 1997). Likewise, transcranial electrical stimulation has been

associated with enhancing motor performance in motor tasks (Spooner and Wilson, 2023) and altering performance in some non-motor tasks (Arif et al., 2021; Erker et al., 2024; McDermott et al., 2019; Wiesman et al., 2018) but not others (Koshy et al., 2020; Spooner et al., 2020). One significant factor that may have contributed to the lack of behavioral findings in this study was the timing of neuromodulation relative to the completion of the motor sequencing task. There is considerable heterogeneity in behavioral effects of transcranial electrical stimulation on motor and cognitive function, particularly with respect to whether the task was completed during stimulation (online effects) or independently (offline effects). Indeed, several studies suggest that behavioral effects are maximal during stimulation or shortly thereafter and reduce in strength over time (Friehs and Frings, 2019; Martin et al., 2014), although others have shown significant stimulation-induced behavioral effects for at least 30 to 45 min or more (Bachtiar et al., 2015; McDermott et al., 2019; Wiesman et al., 2018). Thus, the current behavioral results may not reflect the full magnitude of the neuromodulation effect, which may be more pronounced immediately after stimulation, due to the timing of the MEG task relative to the stimulation. Further work may help elucidate the potential causes of such behavioral inconsistencies in the literature, which may be due, at least in part, to more subtle differences in task design, stimulation parameters and/or configuration, specific brain regions targeted, and/or the participant population of interest.

4.2. Stimulation-by-Task interaction effects

Our most interesting findings were the stimulation-by-task effects in the right dlPFC, a medial area of the left primary motor cortex that bordered the supplemental motor area (SMA), and the right occipitotemporal region. In accordance with our hypothesis that neuromodulation would be dependent on movement complexity, the overall pattern of results suggests that HD-tDCS of the motor cortex affects the beta oscillations serving simple movement sequences, while the same neural responses during performance of complex sequences were unaffected. Indeed, post-hoc testing revealed that anodal stimulation was associated with stronger beta ERD responses during the planning phase of simple trials in each of these three regions relative to both cathodal and sham stimulation, which did not differ from each other in any region. No such stimulation related differences were observed in the complex condition, with the exception of the occipitotemporal region. These results may reflect the utilization of a specialized set of neural resources that are optimized for more advanced motor plans during the complex condition, leading to decreased susceptibility to the effects of stimulation. In contrast, the simple movement plan may be accomplished by using heterogeneous pools of neural resources, leading to more flexibility and thus potential vulnerability to the effects of stimulation. There is at least some support for this perspective in the literature, with a prior rTMS study of the SMA inducing errors only in the more complex movement sequence (Gerloff et al., 1997). Thus, the relative ease of planning simple movements affords a degree of neural flexibility and corollary susceptibility to stimulation that is not observed in complex movement planning, which may require specialized neural mechanisms that are more resistant to perturbation. However, these results should be interpreted with caution and replicated in future studies, as it is also possible that the simple-only effect reflects a limit on the dynamic range of beta responses in the complex condition (Heinrichs-Graham et al., 2018; Wilson et al., 2014; Heinrichs-Graham and Wilson, 2016; Wilson et al., 2018). Taken together, we found that the neural signatures

of movement planning and execution were susceptible to both stimulation polarity and movement complexity in both movement-related and higher-order regions.

4.3. Main effect of task condition

There were several main effects of task condition in the planning and execution periods, replicating a wide body of existing work showing greater neural activity in the complex relative to the simple condition (Haaland et al., 2004; Heinrichs-Graham and Wilson, 2015; Manganotti et al., 1998; McCusker et al., 2021; Shibasaki et al., 1993; Ward et al., 2023). During the planning phase, there were stronger beta ERD responses in the complex condition relative to the simple condition in regions of the right sensorimotor cortices, as well as the right superior parietal lobule. Previous work has identified altered neural activity in the somatosensory cortices well before movement onset (Ariani et al., 2022; Gale et al., 2021), potentially reflecting a preparatory state in anticipation of somatosensory feedback during subsequent execution of the motor plan. In addition, spatial maps in the parietal cortices have been shown to be essential for motor planning and execution, especially in the context of sequence-related movements (Catalan et al., 1998; Haaland et al., 2004; Harrington et al., 2000; Heinrichs-Graham and Wilson, 2015; Manganotti et al., 1998; Turella et al., 2016), with beta band modulations being essential in the planning of such movements. Furthermore, increased beta ERD responses in the complex relative to the simple condition persisted into the execution phase and became more spatially distributed, in line with previous studies showing right parietal cortex activation (Heinrichs-Graham et al., 2020; Heinrichs-Graham and Wilson, 2015). In contrast, the occipito-temporal regions exhibited the opposite effect, where there were stronger beta ERD responses in the simple condition relative to the complex condition. Thus, it appears that while earlier regions in the attention streams and lower-rank components of the sensorimotor-association axis (Sydnor et al., 2021) are sufficient and recruited for simple planning, higher-order parietal and somatosensory regions are preferentially recruited in the complex condition. Taken together, these results point toward regionally specific modulation and recruitment of motor and extrastriate cortices during the performance of motor sequences.

5. Conclusions

These novel contributions to the literature expand upon recent studies and demonstrate the sensitivity of neural processes serving motor control to HD-tDCS in a polarity-dependent manner. Before closing, we want to suggest multiple factors that should be incorporated in future work to broaden the scope of the implications. Though these results contribute significantly to our understanding of how HD-tDCS can impact the neurophysiology underlying movement planning and execution of differing complexities, varying the length of the sequence may also provide overlapping or distinct insights into distinct neurophysiological changes (Catalan et al., 1998). Furthermore, modulation of the stimulation parameters (i.e., amplitude, duration, intermittent or continuous; Hashemirad et al., 2016) may also provide insights into the neurobehavioral impact of noninvasive brain stimulation on motor control. In addition to polarity, the brain state and oscillatory phase during stimulation have also been shown to impact the behavioral effects of neuromodulation, which may further elucidate the mechanisms driving behavioral changes

(Bergmann, 2018; Li et al., 2019; Spooner and Wilson, 2023). Lastly, all of our participants were right-handed according to self-report, but future studies could enhance rigor by performing a formal assessment of handedness. Despite these limitations, the current study provides valuable data on the potential plasticity of the neurophysiology supporting movement planning and execution in healthy adults.

Acknowledgements

This work was supported by the National Institutes of Health [grant numbers RF1-MH117032, S10-OD028751, R01-MH116782, P20-GM144641, F30-MH134713].

Data availability

Data will be made available on request.

References

Antal A, Terney D, Poreisz C, Paulus W, 2007. Towards unravelling task-related modulations of neuroplastic changes induced in the human motor cortex. Eur. J. Neurosci. 26 (9), 2687–2691. [PubMed: 17970738]

Ariani G, Pruszynski JA, Diedrichsen J, 2022. Motor planning brings human primary somatosensory cortex into action-specific preparatory states. Elife 11. 10.7554/eLife.69517.

Arif Y, Spooner RK, Heinrichs-Graham E, 2021. High-definition transcranial direct current stimulation modulates performance and alpha/beta parieto-frontal connectivity serving fluid intelligence. J. Physiol. https://physoc.onlinelibrary.wiley.com/doi/abs/10.1113/JP282387.

Arif Y, Son JJ, Okelberry HJ, Johnson HJ, Willett MP, Wiesman AI, Wilson TW, 2024. Modulation of movement-related oscillatory signatures by cognitive interference in healthy aging. Geroscience. 10.1007/s11357-023-01057-0.

Arif Y, Wiesman AI, Christopher-Hayes N, Okelberry HJ, Johnson HJ, Willett MP, Wilson TW, 2023. Altered age-related alpha and gamma prefrontal-occipital connectivity serving distinct cognitive interference variants. Neuroimage 280, 120351. [PubMed: 37659656]

Avanzino L, Bove M, Trompetto C, Tacchino A, Ogliastro C, Abbruzzese G, 2008. 1-Hz repetitive TMS over ipsilateral motor cortex influences the performance of sequential finger movements of different complexity. Eur. J. Neurosci. 27 (5), 1285–1291. [PubMed: 18312586]

Bachtiar V, Near J, Johansen-Berg H, Stagg CJ, 2015. Modulation of GABA and resting state functional connectivity by transcranial direct current stimulation. Elife 4, e08789. [PubMed: 26381352]

Ballard HK, Eakin SM, Maldonado T, Bernard JA, 2021. Using high-definition transcranial direct current stimulation to investigate the role of the dorsolateral prefrontal cortex in explicit sequence learning. PLoS. One 16 (3), e0246849. [PubMed: 33735211]

Bastani A, Jaberzadeh S, 2014. Within-session repeated a-tDCS: the effects of repetition rate and inter-stimulus interval on corticospinal excitability and motor performance. Clin. Neurophysiol.: Official J. Int. Federation of Clin. Neurophysiol. 125 (9), 1809–1818.

Bergmann TO, 2018. Brain state-dependent brain stimulation. Front. Psychol. 9, 2108. [PubMed: 30443236]

Brinkman L, Stolk A, Dijkerman HC, de Lange FP, Toni I, 2014. Distinct roles for alpha- and beta-band oscillations during mental simulation of goal-directed actions. J. Neurosci.: Off. J. Soc. Neurosci. 34 (44), 14783–14792.

Bush G, Shin LM, 2006. The Multi-Source Interference Task: an fMRI task that reliably activates the cingulo-frontal-parietal cognitive/attention network. Nat. Protoc. 1 (1), 308–313. [PubMed: 17406250]

Bush G, Shin LM, Holmes J, Rosen BR, Vogt BA, 2003. The Multi-Source Interference Task: validation study with fMRI in individual subjects. Mol. Psychiatry 8 (1), 60–70. [PubMed: 12556909]

Catalan MJ, Honda M, Weeks RA, Cohen LG, Hallett M, 1998. The functional neuroanatomy of simple and complex sequential finger movements: a PET study. Brain: J. Neurol. 121 (Pt 2), 253–264.

Churchland MM, Afshar A, Shenoy KV, 2006. A central source of movement variability. Neuron 52 (6), 1085–1096. [PubMed: 17178410]

Convento S, Bolognini N, Fusaro M, Lollo F, Vallar G, 2014. Neuromodulation of parietal and motor activity affects motor planning and execution. Cortex; a JournalDevoted to the Study of the Nervous System and Behavior 57, 51–59.

Datta A, Bansal V, Diaz J, Patel J, Reato D, Bikson M, 2009. Gyri-precise head model of transcranial direct current stimulation: improved spatial focality using a ring electrode versus conventional rectangular pad. Brain Stimul. 2 (4), 201–207, 207.e1. [PubMed: 20648973]

Edwards D, Cortes M, Datta A, Minhas P, Wassermann EM, Bikson M, 2013. Physiological and modeling evidence for focal transcranial electrical brain stimulation in humans: a basis for high-definition tDCS. Neuroimage 74, 266–275. [PubMed: 23370061]

Embury CM, Heinrichs-Graham E, Lord GH, Drincic AT, Desouza CV, Wilson TW, 2019. Altered motor dynamics in type 1 diabetes modulate behavioral performance. NeuroImage. Clinical 24, 101977. [PubMed: 31466021]

Erker TD, Arif Y, John JA, Embury CM, Kress KA, Springer SD, Okelberry HJ, McDonald KM, Picci G, Wiesman AI, Wilson TW, 2024. Neuromodulatory effects of parietal high-definition transcranial direct-current stimulation on network-level activity serving fluid intelligence. J. Physiol. 602 (12), 2917–2930. [PubMed: 38758592]

Ernst MD, 2004. Permutation Methods: A Basis for Exact Inference. Stat. Sci.: Rev. J. Inst. Math. Stat. 19 (4), 676–685.

Friehs MA, Frings C, 2019. Offline beats online: transcranial direct current stimulation timing influences on working memory. Neuroreport 30 (12), 795–799. [PubMed: 31283711]

Gale DJ, Flanagan JR, Gallivan JP, 2021. Human somatosensory cortex is modulated during motor planning. J. Neurosci.: Off. J. Soc. Neurosci. 41 (27), 5909–5922.

Gerloff C, Corwell B, Chen R, Hallett M, Cohen LG, 1997. Stimulation over the human supplementary motor area interferes with the organization of future elements in complex motor sequences. Brain: A Journal of Neurology 120 (9), 1587–1602. [PubMed: 9313642]

Gross J, Kujala J, Hamalainen M, Timmermann L, Schnitzler A, Salmelin R, 2001. Dynamic imaging of coherent sources: Studying neural interactions in the human brain. Proc. Natl. Acad. Sci. u S. a 98 (2), 694–699. [PubMed: 11209067]

Guimarães AN, Porto AB, Marcori AJ, Lage GM, Altimari LR, Alves Okazaki VH, 2023. Motor learning and tDCS: A systematic review on the dependency of the stimulation effect on motor task characteristics or tDCS assembly specifications. Neuropsychologia 179, 108463. [PubMed: 36567006]

Haaland KY, Elsinger CL, Mayer AR, Durgerian S, Rao SM, 2004. Motor sequence complexity and performing hand produce differential patterns of hemispheric lateralization. J. Cogn. Neurosci. 16 (4), 621–636. [PubMed: 15165352]

Hanakawa T, Dimyan MA, Hallett M, 2008. Motor planning, imagery, and execution in the distributed motor network: a time-course study with functional MRI. Cerebral Cortex (New York, N.Y.: 1991) 18 (12), 2775–2788. [PubMed: 18359777]

Harrington DL, Rao SM, Haaland KY, Bobholz JA, Mayer AR, Binderx JR, Cox RW, 2000. Specialized neural systems underlying representations of sequential movements. J. Cogn. Neurosci. 12 (1), 56–77. [PubMed: 10769306]

Hashemirad F, Zoghi M, Fitzgerald PB, Jaberzadeh S, 2016. The effect of anodal transcranial direct current stimulation on motor sequence learning in healthy individuals: A systematic review and meta-analysis. Brain Cogn. 102, 1–12. [PubMed: 26685088]

Heinrichs-Graham E, Arpin DJ, Wilson TW, 2016. Cue-related Temporal Factors Modulate Movement-related Beta Oscillatory Activity in the Human Motor Circuit. J. Cogn. Neurosci. 28 (7), 1039–1051. [PubMed: 26967947]

Heinrichs-Graham E, Kurz MJ, Becker KM, Santamaria PM, Gendelman HE, Wilson TW, 2014. Hypersynchrony despite pathologically reduced beta oscillations in patients with Parkinson's disease: a pharmaco-magnetoencephalography study. J. Neurophysiol. 112 (7), 1739–1747. [PubMed: 25008416]

Heinrichs-Graham E, Kurz MJ, Gehringer JE, Wilson TW, 2017. The functional role of post-movement beta oscillations in motor termination. Brain Struct. Funct. 222 (7), 3075–3086. [PubMed: 28337597]

Heinrichs-Graham E, McDermott TJ, Mills MS, Wiesman AI, Wang Y-P, Stephen JM, Calhoun VD, Wilson TW, 2018. The lifespan trajectory of neural oscillatory activity in the motor system. Dev. Cogn. Neurosci. 30, 159–168. [PubMed: 29525417]

Heinrichs-Graham E, Taylor BK, Wang Y-P, Stephen JM, Calhoun VD, Wilson TW, 2020. Parietal Oscillatory Dynamics Mediate Developmental Improvement in Motor Performance. Cerebral Cortex 30 (12), 6405–6414. [PubMed: 32705142]

Heinrichs-Graham E, Wilson TW, 2015. Coding complexity in the human motor circuit. Hum. Brain Mapp. 36 (12), 5155–5167. [PubMed: 26406479]

Heinrichs-Graham E, Wilson TW, 2016. Is an absolute level of cortical beta suppression required for proper movement? Magnetoencephalographic evidence from healthy aging. Neuroimage 134, 514–521. [PubMed: 27090351]

Heinrichs-Graham E, Wilson TW, Santamaria PM, Heithoff SK, Torres-Russotto D, Hutter-Saunders JAL, Estes KA, Meza JL, Mosley RL, Gendelman HE, 2014. Neuromagnetic evidence of abnormal movement-related beta desynchronization in Parkinson's disease. Cerebral Cortex (New York, N.Y.: 1991) 24 (10), 2669–2678. [PubMed: 23645717]

Hodkinson DJ, Jackson SR, Jung J, 2022. Task-dependent plasticity in distributed neural circuits after transcranial direct current stimulation of the human motor cortex: A proof-of-concept study. Front. Pain. Res. (Lausanne) 3, 1005634. [PubMed: 36506269]

Huang Y, Datta A, Bikson M, Parra LC, 2019. Realistic volumetric-approach to simulate transcranial electric stimulation-ROAST-a fully automated open-source pipeline. J. Neural Eng. 16 (5), 056006. [PubMed: 31071686]

Jurkiewicz MT, Gaetz WC, Bostan AC, Cheyne D, 2006. Post-movement beta rebound is generated in motor cortex: evidence from neuromagnetic recordings. Neuroimage 32 (3), 1281–1289. [PubMed: 16863693]

Kim YK, Park E, Lee A, Im C-H, Kim Y-H, 2018. Changes in network connectivity during motor imagery and execution. PLoS. One 13 (1), e0190715. [PubMed: 29324886]

Klem GH, Lüders HO, Jasper HH, Elger C, 1999. The ten-twenty electrode system of the International Federation. The International Federation of Clinical Neurophysiology. Electroencephalogr. Clin. Neurophysiol. Suppl. 52, 3–6. [PubMed: 10590970]

Koshy SM, Wiesman AI, Spooner RK, Embury C, Rezich MT, Heinrichs-Graham E, Wilson TW, 2020. Multielectrode Transcranial Electrical Stimulation of the Left and Right Prefrontal Cortices Differentially Impacts Verbal Working Memory Neural Circuitry. Cerebral Cortex 30 (4), 2389–2400. [PubMed: 31799616]

Kovach CK, Gander PE, 2016. The demodulated band transform. J. Neurosci. Methods 261, 135–154. [PubMed: 26711370]

Kuo H-I, Bikson M, Datta A, Minhas P, Paulus W, Kuo M-F, Nitsche MA, 2013. Comparing cortical plasticity induced by conventional and high-definition 4 × 1 ring tDCS: a neurophysiological study. Brain Stimul. 6 (4), 644–648. [PubMed: 23149292]

Leite J, Carvalho S, Fregni F, Gonçalves ÓF, 2011. Task-specific effects of tDCS-induced cortical excitability changes on cognitive and motor sequence set shifting performance. PLoS. One 6 (9), e24140. [PubMed: 21909415]

Li LM, Violante IR, Leech R, Ross E, Hampshire A, Opitz A, Rothwell JC, Carmichael DW, Sharp DJ, 2019. Brain state and polarity dependent modulation of brain networks by transcranial direct current stimulation. Hum. Brain Mapp. 40 (3), 904–915. [PubMed: 30378206]

Liebetanz D, Nitsche MA, Tergau F, Paulus W, 2002. Pharmacological approach to the mechanisms of transcranial DC-stimulation-induced after-effects of human motor cortex excitability. Brain: A Journal of Neurology 125 (Pt 10), 2238–2247. [PubMed: 12244081]

Manganotti P, Gerloff C, Toro C, Katsuta H, Sadato N, Zhuang P, Leocani L, Hallett M, 1998. Task-related coherence and task-related spectral power changes during sequential finger movements. Electroencephalogr. Clin. Neurophysiol. 109 (1), 50–62. [PubMed: 11003064]

Maris E, Oostenveld R, 2007. Nonparametric statistical testing of EEG- and MEG-data. J. Neurosci. Methods 164 (1), 177–190. [PubMed: 17517438]

Martin DM, Liu R, Alonzo A, Green M, Loo CK, 2014. Use of transcranial direct current stimulation (tDCS) to enhance cognitive training: effect of timing of stimulation. Exp. Brain Res. 232 (10), 3345–3351. [PubMed: 24992897]

McCusker MC, Wiesman AI, Spooner RK, Santamaria PM, McKune J, Heinrichs-Graham E, Wilson TW, 2021. Altered neural oscillations during complex sequential movements in patients with Parkinson's disease. NeuroImage. Clinical 32, 102892. [PubMed: 34911196]

McDermott TJ, Wiesman AI, Mills MS, Spooner RK, Coolidge NM, Proskovec AL, Heinrichs-Graham E, Wilson TW, 2019. tDCS modulates behavioral performance and the neural oscillatory dynamics serving visual selective attention. Hum. Brain Mapp. 40 (3), 729–740. [PubMed: 30368974]

Nakashima S, Koeda M, Ikeda Y, Hama T, Funayama T, Akiyama T, Arakawa R, Tateno A, Suzuki H, Okubo Y, 2021. Effects of anodal transcranial direct current stimulation on implicit motor learning and language-related brain function: An fMRI study. Psychiatry Clin. Neurosci. 75 (6), 200–207. [PubMed: 33576537]

Ng THB, Sowman PF, Brock J, Johnson BW, 2011. Premovement brain activity in a bimanual load-lifting task. Experimental Brain Research. Experimentelle Hirnforschung. Experimentation Cerebrale 208 (2), 189–201. [PubMed: 21076820]

Nitsche MA, Fricke K, Henschke U, Schlitterlau A, Liebetanz D, Lang N, Henning S, Tergau F, Paulus W, 2003. Pharmacological modulation of cortical excitability shifts induced by transcranial direct current stimulation in humans. J. Physiol. 553 (Pt 1), 293–301. [PubMed: 12949224]

Nitsche MA, Paulus W, 2000. Excitability changes induced in the human motor cortex by weak transcranial direct current stimulation. J. Physiol. 527 (Pt 3), 633–639. Pt 3. [PubMed: 10990547]

Nitsche MA, Paulus W, 2001. Sustained excitability elevations induced by transcranial DC motor cortex stimulation in humans. Neurology. 57 (10), 1899–1901. [PubMed: 11723286]

Nombela-Cabrera R, Pérez-Nombela S, Avendaño-Coy J, Comino-Suárez N, Arroyo-Fernández R, Gómez-Soriano J, Serrano-Muñoz D, 2023. Effectiveness of transcranial direct current stimulation on balance and gait in patients with multiple sclerosis: systematic review and meta-analysis of randomized clinical trials. J. Neuroeng. Rehabil. 20 (1), 142. [PubMed: 37875941]

Notturno F, Marzetti L, Pizzella V, Uncini A, Zappasodi F, 2014. Local and remote effects of transcranial direct current stimulation on the electrical activity of the motor cortical network. Hum. Brain Mapp. 35 (5), 2220–2232. [PubMed: 23913800]

Okamoto M, Dan H, Sakamoto K, Takeo K, Shimizu K, Kohno S, Oda I, Isobe S, Suzuki T, Kohyama K, Dan I, 2004. Three-dimensional probabilistic anatomical cranio-cerebral correlation via the international 10–20 system oriented for transcranial functional brain mapping. Neuroimage 21 (1), 99–111. [PubMed: 14741647]

Okamoto M, Dan I, 2005. Automated cortical projection of head-surface locations for transcranial functional brain mapping. Neuroimage 26 (1), 18–28. [PubMed: 15862201]

Pfurtscheller G, Lopes da Silva FH, 1999. Event-related EEG/MEG synchronization and desynchronization: basic principles. Clinical Neurophysiology: Official Journal of the International Federation of Clinical Neurophysiology 110 (11), 1842–1857. [PubMed: 10576479]

Qiu Y, Yin Z, Wang M, Duan A, Xie M, Wu J, Wang Z, Chen G, 2023. Motor function improvement and acceptability of non-invasive brain stimulation in patients with Parkinson's disease: a Bayesian network analysis. Front. Neurosci. 17, 1212640. [PubMed: 37564368]

Saucedo Marquez CM, Zhang X, Swinnen SP, Meesen R, Wenderoth N, 2013. Task-specific effect of transcranial direct current stimulation on motor learning. Front. Hum. Neurosci. 7, 333. [PubMed: 23847505]

Shibasaki H, Sadato N, Lyshkow H, Yonekura Y, Honda M, Nagamine T, Suwazono S, Magata Y, Ikeda A, Miyazaki M, 1993. Both primary motor cortex and supplementary motor area play an important role in complex finger movement. Brain: A Journal of Neurology 116 (Pt 6), 1387–1398. [PubMed: 8293277]

Son JJ, Arif Y, Okelberry HJ, Johnson HJ, Willett MP, Wiesman AI, Wilson TW, 2024. Aging modulates the impact of cognitive interference subtypes on dynamic connectivity across a distributed motor network. NPJ. Aging 10 (1), 54. [PubMed: 39580466]

Spooner RK, Eastman JA, Rezich MT, Wilson TW, 2020. High-definition transcranial direct current stimulation dissociates fronto-visual theta lateralization during visual selective attention. The Journal of Physiology 598, 987–998. [PubMed: 31840247]

Spooner RK, Taylor BK, Ahmad IM, Dyball KN, Emanuel K, Fox HS, Stauch KL, Zimmerman MC, Wilson TW, 2021. Neural oscillatory activity serving sensorimotor control is predicted by superoxide-sensitive mitochondrial redox environments. Proceedings of the National Academy of Sciences 118 (43), e2104569118.

Spooner RK, Wilson TW, 2023. Spectral specificity of gamma-frequency transcranial alternating current stimulation over motor cortex during sequential movements. Cerebral Cortex 33 (9), 5347–5360. [PubMed: 36368895]

Stagg CJ, Nitsche MA, 2011. Physiological basis of transcranial direct current stimulation. The Neuroscientist: A Review Journal Bringing Neurobiology, Neurology and Psychiatry 17 (1), 37–53. [PubMed: 21343407]

Sutter K, Oostwoud Wijdenes L, van Beers RJ, Medendorp WP, 2021. Movement preparation time determines movement variability. J. Neurophysiol. 125 (6), 2375–2383. [PubMed: 34038240]

Sydnor VJ, Larsen B, Bassett DS, Alexander-Bloch A, Fair DA, Liston C, Mackey AP, Milham MP, Pines A, Roalf DR, Seidlitz J, Xu T, Raznahan A, Satterthwaite TD, 2021. Neurodevelopment of the association cortices: Patterns, mechanisms, and implications for psychopathology. Neuron 109 (18), 2820–2846. [PubMed: 34270921]

Taulu S, Simola J, 2006. Spatiotemporal signal space separation method for rejecting nearby interference in MEG measurements. Phys. Med. Biol. 51 (7), 1759–1768. [PubMed: 16552102]

Taulu S, Simola J, Kajola M, 2005. Applications of the signal space separation method. IEEE Transactions on Signal Processing: A Publication of the IEEE Signal Processing Society 53 (9), 3359–3372.

Toni I, Krams M, Turner R, Passingham RE, 1998. The time course of changes during motor sequence learning: a whole-brain fMRI study. Neuroimage 8 (1), 50–61. [PubMed: 9698575]

Turella L, Tucciarelli R, Oosterhof NN, Weisz N, Rumiati R, Lingnau A, 2016. Beta band modulations underlie action representations for movement planning. Neuroimage 136, 197–207. [PubMed: 27173760]

Tzagarakis C, Ince NF, Leuthold AC, Pellizzer G, 2010. Beta-band activity during motor planning reflects response uncertainty. J. Neurosci.: Off. J. Soc. Neurosci. 30 (34), 11270–11277.

Uusitalo MA, Ilmoniemi RJ, 1997. Signal-space projection method for separating MEG or EEG into components. Med. Biol. Eng. Comput. 35 (2), 135–140. [PubMed: 9136207]

van Beers RJ, Haggard P, Wolpert DM, 2004. The role of execution noise in movement variability. J. Neurophysiol. 91 (2), 1050–1063. [PubMed: 14561687]

Van Veen BD, van Drongelen W, Yuchtman M, Suzuki A, 1997. Localization of brain electrical activity via linearly constrained minimum variance spatial filtering. IEEE Trans. Biomed. Eng. 44 (9), 867–880. [PubMed: 9282479]

Wang S-M, Chan Y-W, Tsui Y-O, Chu F-Y, 2021. Effects of Anodal Cerebellar Transcranial Direct Current Stimulation on Movements in Patients with Cerebellar Ataxias: A Systematic Review. Int. J. Environ. Res. Public Health 18 (20). 10.3390/ijerph182010690.

Ward TW, Springer SD, Schantell M, John JA, Horne LK, Coutant AT, Okelberry HJ, Willett MP, Johnson HJ, Killanin AD, Heinrichs-Graham E, Wilson TW, 2023. Regular cannabis use alters the neural dynamics serving complex motor control. Hum. Brain Mapp. 44 (18), 6511–6522. [PubMed: 37955378]

Wiesman AI, Koshy SM, Heinrichs-Graham E, Wilson TW, 2020. Beta and gamma oscillations index cognitive interference effects across a distributed motor network. Neuroimage 213, 116747. [PubMed: 32179103]

Wiesman AI, Mills MS, McDermott TJ, Spooner RK, Coolidge NM, Wilson TW, 2018. Polarity-dependent modulation of multi-spectral neuronal activity by transcranial direct current stimulation. Cortex 108, 222–233. [PubMed: 30261367]

Wiesman AI, Wilson TW, 2020. Attention modulates the gating of primary somatosensory oscillations. Neuroimage 211, 116610. [PubMed: 32044438]

Wiesman AI, Wilson TW, 2020. Posterior Alpha and Gamma Oscillations Index Divergent and Superadditive Effects of Cognitive Interference. Cerebral Cortex 30 (3), 1931–1945. [PubMed: 31711121]

Wilson TW, Heinrichs-Graham E, Becker KM, 2014. Circadian modulation of motor-related beta oscillatory responses. Neuroimage 102 (02), 531–539. Pt 2. [PubMed: 25128712]

Wilson TW, Heinrichs-Graham E, Proskovec AL, McDermott TJ, 2016. Neuroimaging with magnetoencephalography: A dynamic view of brain pathophysiology. Transl. Res. J. Lab. Clin. Med. 175, 17–36.

Wilson TW, McDermott TJ, Mills MS, Coolidge NM, Heinrichs-Graham E, 2018. tDCS modulates visual gamma oscillations and basal alpha activity in occipital cortices: evidence from MEG. Cereb Cortex 28 (5), 1597–1609. [PubMed: 28334214]

Wilson TW, Heinrichs-Graham E, Robertson KR, Sandkovsky U, O'Neill J, Knott NL, Fox HS, Swindells S, 2013. Functional brain abnormalities during finger-tapping in HIV-infected older adults: a magnetoencephalography study. J. Neuroimmune Pharmacol.: The Official Journal of the Society on NeuroImmune Pharmacology 8 (4), 965–974.

Wilson TW, Slason E, Asherin R, Kronberg E, Reite ML, Teale PD, Rojas DC, 2010. An extended motor network generates beta and gamma oscillatory perturbations during development. Brain Cogn. 73 (2), 75–84. [PubMed: 20418003]

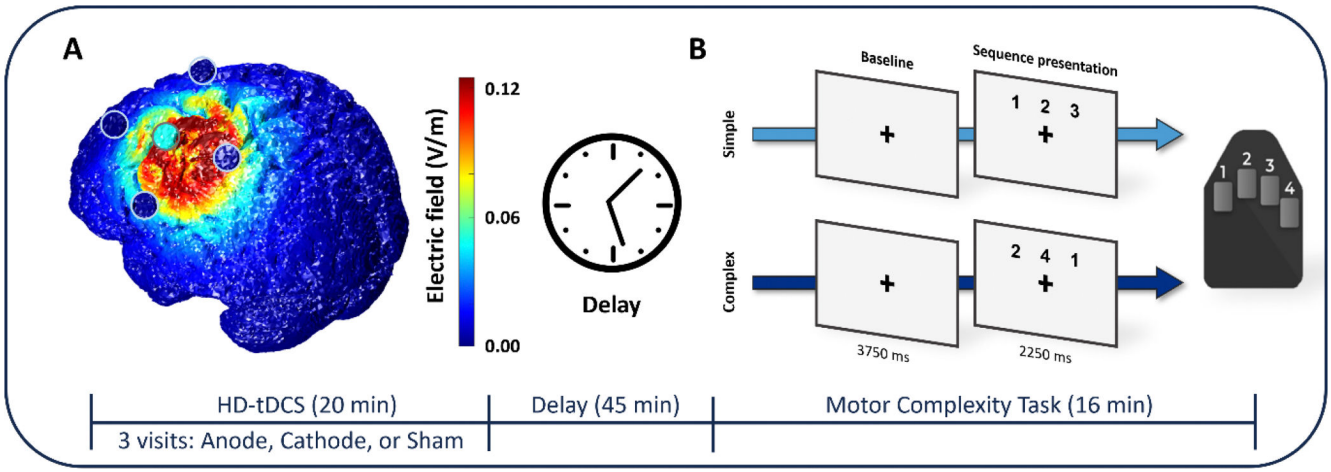

Fig. 1. Current flow model and experimental protocol.

(A) Current distribution modeling using the HD-tDCS montage showed relatively focal stimulation of the left primary motor cortex. Participants received 20 min of anodal, cathodal, and sham HD-tDCS over the left primary motor cortex during three sessions, which were pseudorandomized and separated by at least a week (mean = 9.77 days). Following stimulation, there was a 45-minute average delay during which the HD-tDCS equipment was removed from the participant's head and they were prepared and positioned for the MEG recording. (B) Participants completed a motor sequencing task during the MEG recording, which consisted of a fixation cross for 3750 ms, followed by a series of three numbers with each corresponding to a finger on their right hand. Participants were instructed to quickly and accurately press the buttons corresponding to the sequence, prior to the sequence disappearing after 2250 ms. There were two conditions that were distinguished by the complexity of the motor plan. In the "simple" condition, the series of numbers in the plan were sequential and resulted in the tapping of 3 adjacent fingers, while in the "complex" condition each number was at least one number away from the previous number, and thus mapped to a sequence in which the finger being tapped was not adjacent to the previous finger tapped.

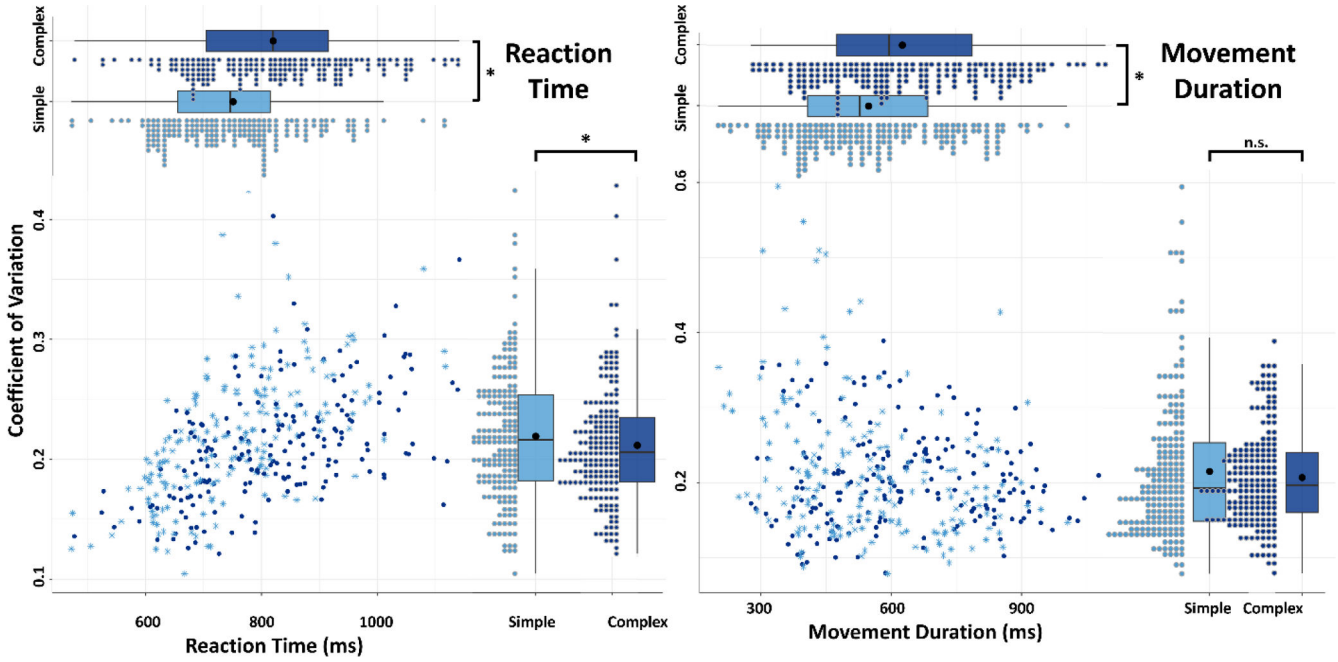

Fig. 2. Behavioral performance on the motor sequencing task.

The scatterplots show reaction time (left) and movement duration (right) on the x-axis and the coefficient of variation on the y-axis, with each datapoint reflecting the behavioral outcome in either the simple (light blue) or complex (dark blue) condition. Box plots *above* the scatterplots represent the data distributions for reaction time and movement duration, while the box plots to the *right* of the scatterplots represent the data distributions of measure variability. * indicates $p < .05$, n.s. indicates not significant.

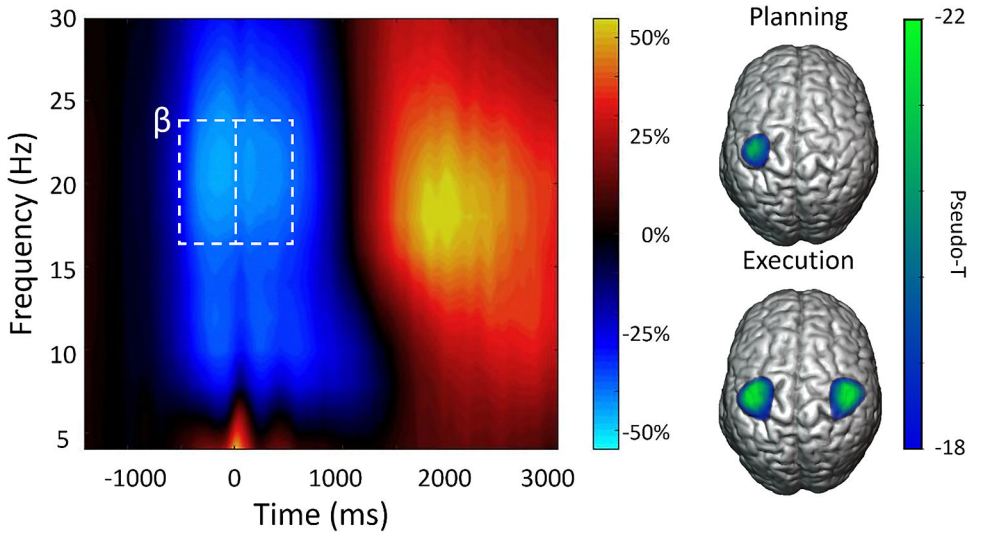

Fig. 3. Sensor- and source-level responses to the motor sequencing task.

The grand-averaged time-frequency spectrogram from a MEG sensor near the motor cortices with time (ms) displayed on the x-axis and frequency (Hz) on the y-axis, with the color bar representing the percent difference in power from baseline. Dashed boxes indicate statistically significant decreases in beta power that were subjected to beamforming. On the right, grand-averaged beamformer images (across both task conditions and the three stimulation conditions) are shown for the planning and execution time-frequency windows.

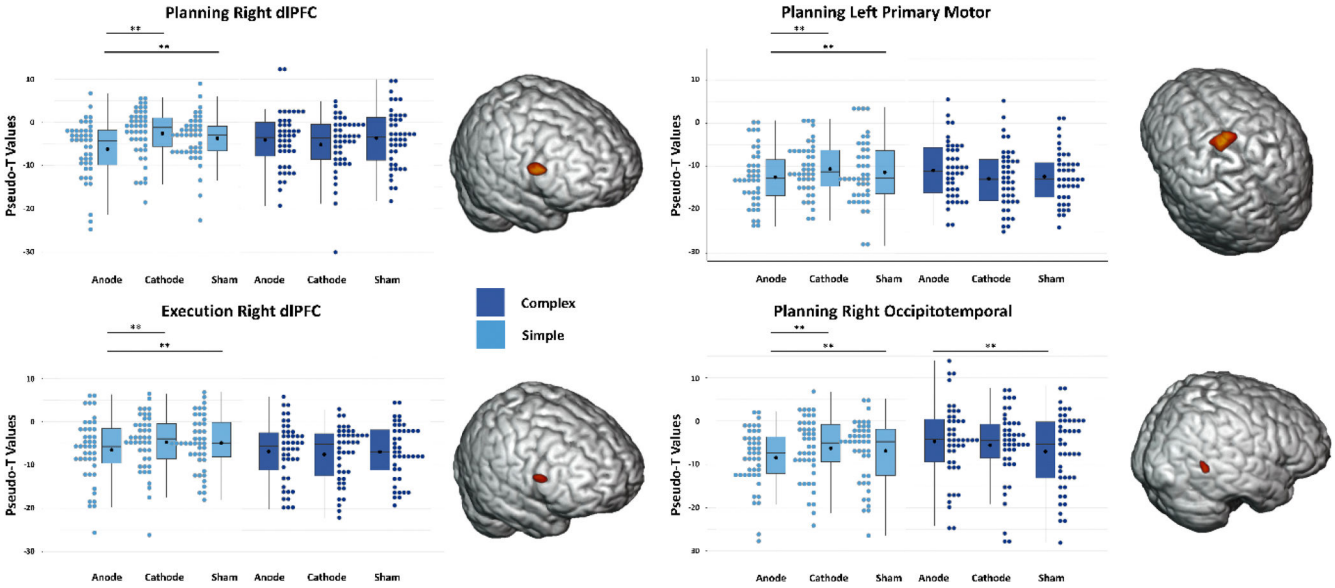

Fig. 4. Stimulation-by-task interaction effects in the planning and execution windows.

Whole-brain 2 × 3 repeated-measures ANOVAs revealed significant stimulation-by-task interaction effects (all *p*s < .001). The histograms show the median (black line) and mean (black dot), as well as the individual data points for each of the stimulation and task conditions. In the planning window, there were significant interactions in the right occipitotemporal cortex, dorsolateral prefrontal cortex (dlPFC), and a left primary motor cortex area directly posterior to the supplemental motor area (SMA). In the execution window, there was a significant interaction in the right dlPFC. Stronger beta oscillatory responses (i.e., more negative relative to baseline) during the planning phase were observed in the simple condition following anodal stimulation compared to cathodal and sham in all three regions and the same pattern held for beta responses during movement execution in the right dlPFC. Finally, weaker beta oscillations were observed following anodal stimulation compared to the sham condition in the right occipitotemporal cortex. $^{**}p < .005$, $^{*}p < .05$.

Table 1

Reaction Time (ms).

Condition	Anode	Cathode	Sham	Mean
Simple	755.5 (169.5)	754.6 (171.7)	743.7 (163.9)	751.2 (168.4)
Complex	831.1 (180.8)	822.1 (179.5)	808.0 (170.4)	820.4 (176.9)
Mean	793.3 (175.2)	788.3 (175.6)	775.8 (167.2)	785.8 (172.7)
*Movement Duration (*ms*)*				
Simple	556.7 (117.4)	552.5 (111.7)	537.8 (110.1)	549.0 (113.1)
Complex	637.5 (134.6)	622.5 (127.2)	619.9 (125.1)	626.7 (129.0)
Mean	597.1 (126.0)	587.5 (119.5)	578.8 (117.6)	587.8 (121.0)
Accuracy (%)				
Simple	95.3	95.2	95.7	95.4
Complex	94.5	94.0	95.2	94.6
Mean	94.9	94.6	95.5	94.0

Reaction time and movement duration values presented as: mean (SD).